Sensors and Materials, Vol. 29, No. 9 (2017) 1241–1246
MYU Tokyo

S & M 1416

Improved Sensitivity of Microring Resonator-Loaded Mach–Zehnder Interferometer Biosensor

Soichiro Yoshida, Shintaro Ishihara, Yoshiaki Nishijima, Yasuo Kokubun, and Taro Arakawa*

Graduate School of Engineering, Yokohama National University
79-5 Tokiwadai, Hodogaya-ku, Yokohama, Kanagawa 240-8501, Japan

(Received March 1, 2017; accepted May 2, 2017)

Keywords: biosensor, microring resonator, Mach–Zehnder interferometer, biotin, variable optical attenuator

We investigated the improvement in the sensitivity of a biosensor based on a silicon microring resonator-loaded Mach–Zehnder interferometer (MRR-MZI). Thermo-optic-driven variable optical attenuators (VOAs) were used to balance the optical power in one arm with that in the other to obtain a high extinction ratio of the MRR-MZI. The change in the transmittance as large as 12.9 and 7.5 dB for the detection of 200 and 20 pM avidin, respectively, was successfully obtained. These values are larger than those observed before the adjustment of the optical power balance by 4.8 and 5.3 dB, respectively. We discuss the characteristics of light power adjustment of the VOA and confirmation of biotin modification of the surface of the silicon waveguide using fluorescein-polyethylene glycol-*N*-hydroxylsuccinimide (fluorescein-PEG-NHS).

1. Introduction

Label-free optical biosensing is a highly important technology for the detection of specific biomolecules such as DNA and proteins. As high-sensitivity label free sensors, surface plasmon resonance (SPR) sensors[1–3] have been developed and used for various applications including medical diagnostics. Lately, as more compact optical biosensors with simpler structures, biosensors based on photonic devices have been proposed.[4–11] In addition, microring resonator (MRR)-based biosensors have also been intensively developed because of their compactness, high sensitivity, and low cost.[12–20] We have also proposed and developed a biosensor based on an MRR-loaded Mach–Zehnder interferometer (MRR-MZI)[21] that has a higher sensitivity than conventional MRR sensors. Although avidin at a concentration as low as 20 pM was detected as a change in light transmittance with the MRR-MZI sensor, a sufficient change in transmittance has not yet been obtained.

In this study, we investigated the improvement of the sensitivity of the MRR-MZI by using variable optical attenuators (VOAs) to balance the optical power in one arm with that in the other. The change in light transmittance of the MRR-MZI was significantly increased. We discuss the characteristics of light power adjustment of the VOA and confirm the biotin modification of the surface of the sample using fluorescein-polyethylene glycol-*N*-hydroxylsuccinimide (fluorescein-PEG-NHS).

*Corresponding author: e-mail: arakawa-taro-vj@ynu.ac.jp
http://dx.doi.org/10.18494/SAM.2017.1587

ISSN 0914-4935

2. Structure and Sensing Principle of MRR-MZI Sensor

Figure 1 shows a micrograph of the MRR-MZI biosensor. The MRR is coupled with one arm through a directional coupler (DC). The optical power coupling efficiency K is designed to be 0.2. The waveguides are Si wires 210 nm high and 400 nm wide. The round-trip length is designed to be 69.3 μm. The Si waveguides, except for those of the MRR and DC, are buried in SiO_2 cladding layers. Upper and side cladding layers of the MRR and DC are removed, and the MRR functions as a sensing part. 1 × 2 multimode interference (MMI) 3 dB couplers are used in the Mach–Zehnder interferometer (MZI) for input and output ports. The MZI has MZI-based VOAs in both arms to adjust the balance between the optical powers in both arms for a higher extinction ratio. Although each arm is also equipped with a phase shifter driven by a heater, the phase shifters were not used in this experiment. The MRR-MZI sensors were fabricated on a silicon-on-insulator (SOI) substrate using a CMOS-compatible process.

Figure 2 shows the calculated effective phase shift φ_{eff} caused by the resonance in the MRR for various values of K versus the single-pass phase shift φ for a silicon MRR with a round-trip length of 69.3 μm. The propagation loss in the MRR is assumed to be 1.22 dB/cm. The nonlinear change in φ_{eff} is strongly enhanced in the vicinity of the on-resonance state $\varphi = 0$.[21] The nonlinearity in φ_{eff} is enhanced as K decreases. Owing to the enhanced φ_{eff}, even a small change in the environmental refractive index results in a large φ_{eff}.

By changing the difference in phases between the lightwaves in both arms, the transmittance between input and output ports of the MZI is changed. When a protein is adsorbed on the top and sidewalls of the waveguide of the MRR, the equivalent refractive index of the waveguide changes, leading to a large change in φ_{eff}. The transmittance of the MZI is markedly changed even by the enhanced change in φ_{eff}, even if the change in the environmental refractive index is small. As a result, the MZI functions as a high-sensitivity protein sensor.

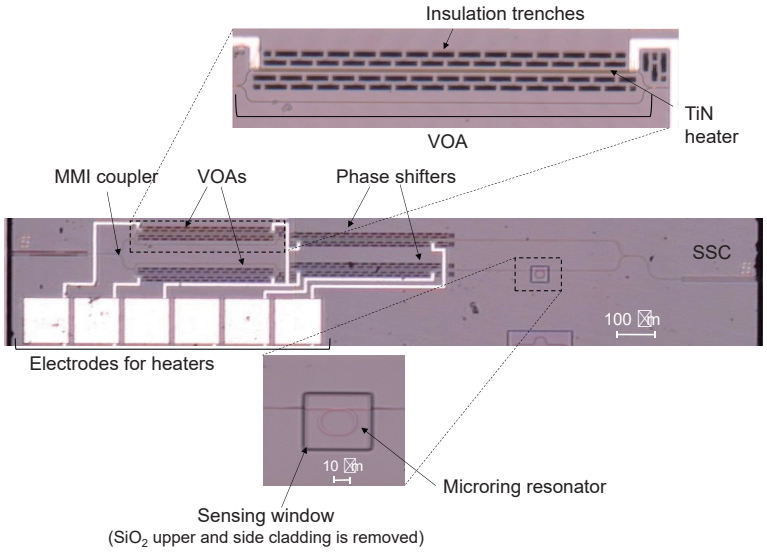

Fig. 1. (Color online) Micrograph of the MRR-MZI biosensor with VOAs.

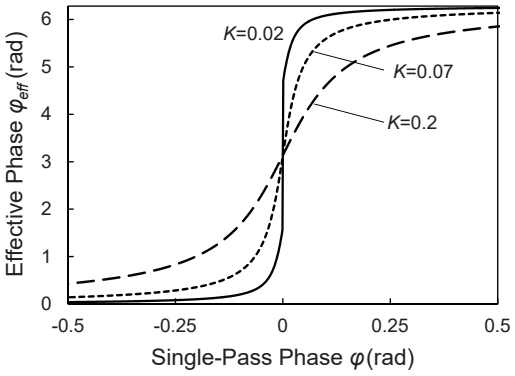

Fig. 2. Calculated effective phase shift φ_{eff} caused by the resonance in the MRR for various values of K versus the single-pass phase shift φ for a silicon MRR with a round-trip length of 69.3 μm.

3. Experimental Results

First, the attenuation characteristics of the VOA were measured. The VOA consists of an MZI with a TiN heater on top of the Si waveguide. Owing to the thermo-optic (TO) effect of Si, the refractive index of the waveguide of one arm is changed by the heater, and the transmittance of the MZI can be adjusted. Figure 3 shows the dependence of the transmittance on the electric power supplied to the heater. The transmittance is successfully changed by an electric power of a few tens of watts. Note that it takes some time for the VOA to attain a stable state. Figure 4 shows the temporal change in transmittance spectra after light power adjustment using the VOA. The stable state is obtained in approximately 15 min. Even though isolation trenches are formed around the VOAs, the heat generated at the VOAs is slightly leaked and conducted to the MRR. This results in the temporal change in the transmission characteristics. In the following experiments, the sensing characteristics were measured after the VOA became stable.

We investigated the sensing characteristics for avidin solutions to demonstrate protein detection. Biotin-polyethylene glycol-*N*-hydroxylsuccinimide (biotin-PEG-NHS) is fixed on the surface of the Si waveguide followed by the adsorption of avidin on the surface of the waveguide through host–guest specific binding between avidin and biotin. The detailed procedure is described in Ref. 21.

To confirm the modification of the surface of the sample with biotin, the surface was modified with fluorescein-PEG-NHS and observed by fluorescence microscopy. First, fluorescence at a wavelength around 520 nm from the surface was observed, as shown in Fig. 5(a). Next, an octagonal excitation light was shone on the surface. As a result, fading of the fluorescence was observed, as shown in Fig. 5(b), demonstrating that the surface of the sample was successfully fixed by fluorescein-PEG-NHS. This result indicates that it is possible to fix biotin-PEG-NHS, in which fluorescein is replaced by biotin, on the sample.

The transmittances of laser light with transverse electric (TE) polarization before and after adsorption of avidin on the surface of the MRR waveguide were measured using an optical spectrum analyzer. The MRR-MZI chip has silica spot size converters (SSCs) with Si inverse taper waveguides and deep trenches as input and output ports. The width and height of the SSCs are both 4 mm. Single-mode optical fibers (mode field diameter: 10.5 μm) are aligned with the SSCs.

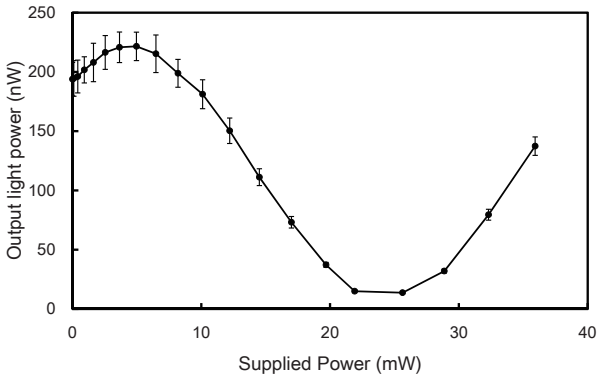

Fig. 3. Dependence of the light transmittance of the VOA on the electric power supplied to the TiN heater.

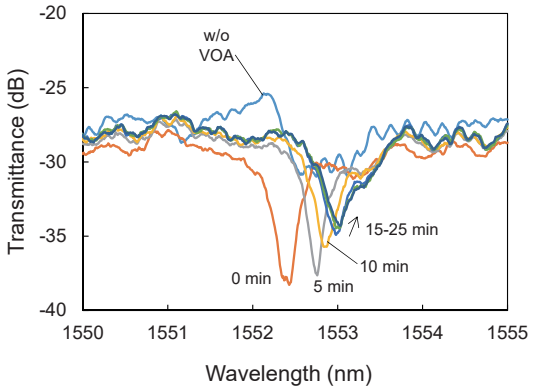

Fig. 4. (Color online) Temporal change in transmittance spectra after light power adjustment using the VOA.

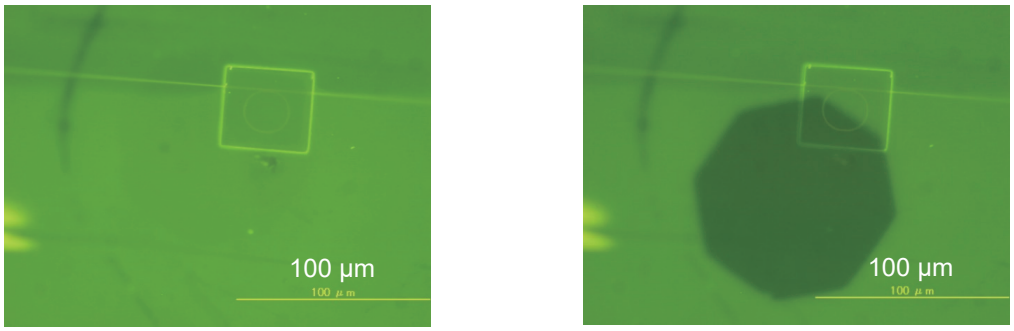

(a) (b)

Fig. 5. (Color online) Micrographs of (a) fluorescence at a wavelength around 520 nm from the surface of the sample and (b) fading of the fluorescence after irradiation by an octagonal excitation light.

Figures 6(a) and 6(b) show the measured transmission spectra of the MRR-MZI for 200 and 20 pM avidin solutions, respectively. In both cases, the optical power balance was adjusted using the VOAs. The spectrum before adjustment by the VOA is also shown in Fig. 6(a). In the case of the 200 pM solution, the resonant wavelength was shifted by 122 pM and the transmittance at 1535.79 nm was changed by 12.9 dB. In the case of the 20 pM solution, the resonant wavelength was shifted by 92 pM after avidin adsorption, and the transmittance at 1552.97 nm was changed by 7.5 dB. The changes in transmittance were increased by 4.8 and 5.3 dB, respectively, compared with that before the adjustment of the optical power balance.[21] These results indicate that the MRR-MZI is very promising as a biosensor, and sensitivity as high as 1 pM may be expected if the power balance is adjusted more precisely using both the VOAs and phase shifters. The coupling efficiency K and the Q factor of the MRR evaluated from the transmission spectra are 0.07 and 1.247×10^4, respectively. This coupling efficiency was smaller than the designed value of 0.2 because of fabrication errors, leading to better performance of the fabricated device than that of the designed one. We selected the designed value of K as a sufficiently large value for satisfying the overcoupling condition where K needs to be larger than 0.02.

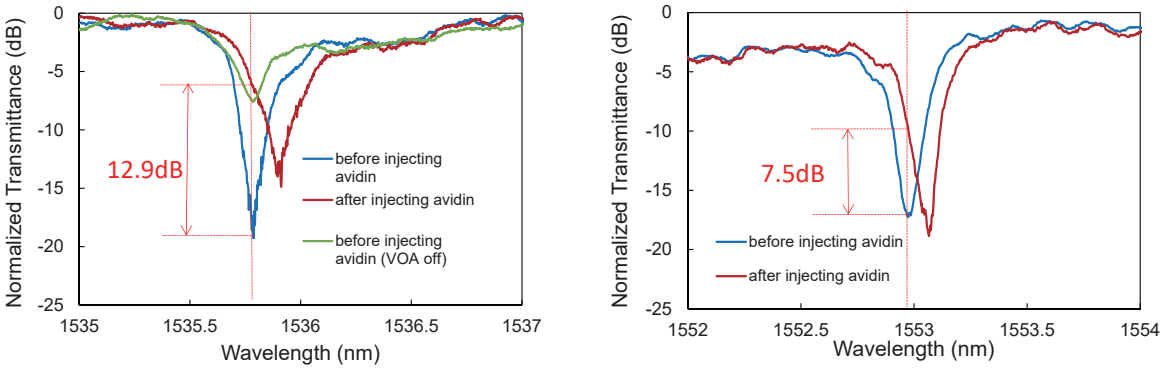

Fig. 6. (Color online) Measured transmission spectra of the MRR-MZI for avidin solutions with the concentrations (a) 200 and (b) 20 pM. The spectrum before adjustment by the VOA is also shown in (a).

4. Conclusions

We investigated the improvement in the sensitivity of an MRR-MZI using TO-driven VOAs. To balance the optical power in one arm with that in the other using the VOAs, the change in transmittance of 12.9 and 7.5 dB for the detection of 200 and 20 pM avidin, respectively, was successfully obtained. These values are larger than those before the adjustment of the optical power balance by 4.8 and 5.3 dB, respectively. These results show that a Si MRR-MZI is promising as a highly sensitive biosensor.

Acknowledgments

The authors express their sincere thanks to Prof. Toshio Ogino, Yokohama National University, for his support of the experiments. This work was partly supported by a Grant-in-Aid for Scientific Research B (No. 15H03577) from the Ministry of Education, Culture, Sports, Science and Technology and by Fujikura Foundation.

References

1 J. Homola: Chem. Rev. **108** (2008) 462.
2 H. Vaisocherová, H. Šípová, I. Víšová, M. Bocková, T. Špringer, M. Ermini, X. Song, Z. Krejčík, L. Chrastinová, O. Pastva, K. Pimková, M. Merkerová, J. Dyr, and J. Homola: Biosens. Bioelectron. **70** (2015) 226.
3 A. Olaru, C. Bala, N. Jaffrezic-Renault, and H. Aboul-Enei: Crit. Rev. Anal. Chem. **45** (2015) 97.
4 G. Cross, A. Reeves, S. Brand, J. Popplewell, L. Peel, M. Swann, and N. Freeman: Biosens. Bioelectron. **19** (2003) 383.
5 C. Barrios, M. Banuls, V. Gonzalez-Pedro, K. Gylfason, B. Sanchez, A. Griol, A. Maquieira, H. Sohlstrom, M. Holgado, and R. Casquel: Opt. Lett. **33** (2008) 708.
6 S. Kita, K. Nozaki, and T. Baba: Opt. Express **16** (2008) 8174.
7 D. Dorfner, T. Zabel, T. Hürlimann, N. Hauke, L. Frandsen, U. Rant, G. Abstreiter, and J. Finley: Biosens. Bioelectron. **29** (2009) 3688.
8 S. Hachuda, S. Otsuka, S. Kita, T. Isono, M. Narimatsu, K. Watanabe, Y. Goshima, and T. Baba: Opt. Express **21** (2013) 12815.

9 W. Chen, Z. Meng, M. Xue, and K. Shea: Mol. Imprinting **4** (2016) 1.
10 K. Uchiyamada, K. Okubo, M. Yokokawa, E. Carlen, K. Asakawa, and H. Suzuki: Opt. Express **23** (2015) 17156.
11 L. Luo, G. Feng, S. Zhou, and T. Tang: Optik **127** (2016) 4019.
12 A. Ramachandran, S. Wang, J. Clarke, S. Ja, D. Goad, L. Wald, E. Flood, E. Knobbe, J. Hryniewicz, S. Chu, D. Gill, W. Chen, O. King, and B. Little: Biosens. Bioelectron. **23** (2008) 939.
13 K. Vos, I. Bartolozzi, E. Schacht, P. Bienstman, and R. Baets: Opt. Express **15** (2007) 7610.
14 S. Yamatogi, Y. Amemiya, T. Ikeda, A. Kuroda, and S. Yokoyama: Jpn. J. Appl. Phys. **48** (2009) 04C188.
15 M. Luchansky, A. Washburn, T. Martin, M. Iqbal, L. Gunn, and R. Bailey: Biosens. Bioelectron. **26** (2010) 1283.
16 M. Li, Y. Liu, Y. Chen, and J. He: J. Phys.: Conf. Ser. **680** (2016) 012004.
17 E. Valera, W. Shia, and R. Bailey: Clin. Biochem. **49** (2016) 121.
18 M. Jäger, T. Becherer, J. Bruns, R. Haag, and K. Petermann: Sens. Actuators, B **223** (2016) 400.
19 F. Meziane, V. Raimbault, H. Hallil, S. Joly, V. Conédéra, J. Lachaud, L. Béchou, D. Rebière, and C. Dejous: Sens. Actuators, B **209** (2015) 1049.
20 A. Samusenko, D. Gandolfi, G. Pucker, T. Chalyan, R. Guider, M. Ghulinyan, and L. Paves: J. Lightwave Technol. **34** (2016) 969.
21 S. Yoshida, S. Ishihara, T. Arakawa, and Y. Kokubun: Jpn. J. Appl. Phys. **56** (2017) 04CH08.